Biomaterials Science

Thermally-modulated cell separation columns using a thermoresponsive block copolymer brush as a packing material for the purification of mesenchymal stem cells

Journal:	*Biomaterials Science*
Manuscript ID	BM-ART-05-2021-000708.R1
Article Type:	Paper
Date Submitted by the Author:	29-Jun-2021
Complete List of Authors:	Nagase, Kenichi; Keio University, Faculty of Pharmacy Edatsune, Goro; Keio University, Faculty of Pharmacy Nagata, Yuki; Keio University, Faculty of Pharmacy Matsuda, Junnosuke; Keio University Ichikawa, Daiju; Keio University, Faculty of Pharmacy Yamada, Sota; Keio University, Faculty of Pharmacy Hattori, Yutaka; Keio University, Faculty of Pharmacy Kanazawa, Hideko; Keio University, Faculty of Pharmacy

Thermally-modulated cell separation columns using a thermoresponsive block copolymer brush as a packing material for the purification of mesenchymal stem cells

Kenichi Nagase*[,a] Goro Edatsune [a], Yuki Nagata [a], Junnosuke Matsuda [a], Daiju Ichikawa [a]

Sota Yamada [a], Yutaka Hattori [a], Hideko Kanazawa [a]

[a]Faculty of Pharmacy, Keio University, 1-5-30 Shibakoen, Minato, Tokyo 105-8512, Japan

*Corresponding author Tel: +81-3-5400-1378; Fax: +81-3-5400-1378

E-mail: nagase-kn@pha.keio.ac.jp

Abstract

Cell therapy using mesenchymal stem cells (MSCs) is used as effective regenerative therapy. Cell therapy requires effective cell separation without cell modification and cellular activity reduction. In this study, we developed a temperature-modulated mesenchymal stem cell separation column. A temperature-responsive cationic block copolymer, poly(*N,N*-dimethylaminopropylacrylamide)-*b*-poly(*N*-isopropylacrylamide)(PDMAPAAm-*b*-PNIPAAm) brush with various cationic copolymer compositions, was grafted on silica beads through two steps of atom transfer radical polymerization. Using the packed beads, the elution behavior of the MSCs was observed. At 37°C, the MSCs were adsorbed on the column through both hydrophobic and electrostatic interactions with the PNIPAAm and PDMAPAAm segments of the copolymer brush, respectively. By reducing the temperature to 4°C, the adsorbed MSCs were eluted from the column by reducing the hydrophobic and electrostatic interactions attributed to the hydration and extension of the PNIPAAm segment of the block copolymer brush. From the temperature-modulated adsorption and elution behavior of MSCs, a suitable DMAPAAm composition in block copolymer brush was determined. Using the column, a mixture of MSC and BM-$CD34^+$ cells was separated by simply changing the column temperature. The column purified the MSCs from the purity of 47.7% to 78.2% through a temperature change from 37°C to 4°C. Additionally, cellular activity of MSCs was maintained through the column separation step. Overall, the obtained results showed that the developed column can be useful for MSC separation without cell modification and cellular activity reduction.

Keywords: Thermoresponsive polymer, Cell separation, Polymer brush, Temperature-responsive chromatography, Stem cell

1. Introduction

Regenerative therapy by transplanting cell suspensions or cellular tissues to patients has become among the effective cures for intractable diseases.[1-6] Especially, regenerative therapy using mesenchymal stem cells (MSCs) has been attracting attention as effective cell therapy.[7-9] MSCs secretes various types of cytokines, leading to improve function of damaged tissues.[10-15] Further, MSCs could be used in various types of stem cell based gene therapies.[16, 17]

In such kinds of therapy, cell separation is an essential protocol for the preparation of cell suspensions or the fabrication of cellular tissues, as MSCs are mixed with other types of cells in human body tissues. To date, various types of cell separation techniques have been developed.[18-27] Among them, cell separation methods that include the modification of fluorescent-labeled antibodies or magnetic beads to cell surfaces have been widely used as precise cell separation techniques. However, the cell surface modification in separation techniques can reduce the intrinsic properties of cells, thus reducing their therapeutic effect. Therefore, cell separation techniques without the modification of cell surfaces are significantly required for cell therapy applications.

Recently, cell separation using poly(*N*-isopropylacrylamide)(PNIPAAm) has been investigated as a cell separation technique that does not entail the modification of cell surfaces.[28-34] PNIPAAm exhibited a temperature-dependent hydrophilic/hydrophobic property change attributed to hydration and dehydration, and PNIPAAm exhibited extension and shrinking. The unique property of PNIPAAm was utilized in various types of biomedical applications, such as temperature-modulated drug delivery systems,[35-38] PNIPAAm-conjugated proteins with temperature-modulated protein function changes, [39-41] biosensors, bioimaging system responses with external temperature changes,[42-46] chromatographic separation systems using the all-aqueous mobile phase,[47-49] and cell culture substrates for fabricating cellular tissues.[50-54] In the cell separation systems that use PNIPAAm, cells are attached to

PNIPAAm-modified glass surfaces at 37°C, as the modified PNIPAAm on the glass become hydrophobic, and the cells tend to be attached to the PNIPAAm surface. By reducing the temperature to 20°C, the attached cells are detached from the surfaces, as the modified PNIPAAm become hydrophilic due to hydration, and cells cannot attach to hydrophilic surfaces.

The differences in the attachment and detachment properties of the cells were utilized for cell separation. For example, a mixture of myoblast and endothelial cells was separated using PNIPAAm-modified surfaces.[29] To increase the selectivity in the cell attachment, the ionic PNIPAAm copolymer-modified surfaces were investigated. For example, using the PNIPAAm copolymers with the anionic groups, smooth muscle cells were separated from the endothelial cells.[55] Additionally, selective adhesion and detachment of MSCs were performed using cationic PNIPAAm copolymer.[56, 57] In addition, micro/nano-imprinted substrates grafted with PNIPAAm was utilized to increase the difference in the cell adhesion properties among the fibroblasts, endothelial cells, and smooth muscle cells, leading to cell separation selectivity.[32] These separation techniques separate cells by changing the temperature without modifying the cells. However, they use PNIPAAm copolymer-modified flat glass substrates or polymer film substrates, which have limited surface area for cell attachment, leading to a limited amount of cell separation.

To overcome the above-mentioned problem, in this study, we developed a thermoresponsive cell separation column using PNIPAAm cationic block copolymer brush-modified beads as packing materials. Silica beads grafted with a block copolymer brush composed of cationic bottom segments and thermoresponsive upper segments were prepared through two steps of surface-initiated atom transfer radical polymerization (ATRP). The cationic segment composition of the modified block copolymer brush was determined by observing the temperature-dependent cell elution behavior of the column. Using the beads packing column, the temperature-modulated separation of the MSCs from the bone

marrow cells was simply performed by changing the temperature while maintaining the cellular activity without the modification of the cell surfaces.

2. Materials and Methods

2.1 Materials

N-isopropylacrylamide (NIPAAm) and *N,N*-dimethylaminopropylacrylamide (DMAPAAm) were provided by KJ Chemicals (Tokyo, Japan), and NIPAAm was recrystallized from *n*-hexane. DMAPAAm was purified by distillation. Tris(2-aminoethyl)amine, formaldehyde, formic acid, sodium hydroxide, dichloromethane, magnesium sulfate, hydrochloride, acetone, 2-propanol, and copper (I) chloride were obtained from Fujifilm Wako Pure Chemical Corporation (Osaka, Japan). α-chloro-*p*-xylene was obtained from Tokyo Chemical Industries (Tokyo, Japan), and ([Chloromethyl]phenylethyl) trimethoxysilane (CPTMS) was obtained from Gelest (Morrisville, PA, USA). Tris[(2-dimethylamino)ethyl]amine (Me_6TREN) was synthesized from TREN.[58] Silica beads (Wakosil® C-200, pore diameter: 6 nm, surface area: 475 m^2/g) were obtained from Fujifilm Wako Pure Chemical Corporation (Osaka, Japan). Porous silica beads were used in the present study because they are primarily used in sample preparation in chromatography and modification condition can be easily determined from the previous reports.[59-62] Extract-Clean empty column was obtained from Systech (Tokyo, Japan), and MSC were obtained from the JCRB cell bank (Osaka, Japan) and Promocell (Heidelberg, Germany). Bone marrow $CD34^+$ Cells (BM-$CD34^+$) and normal human dermal fibroblasts (NHDF) were obtained from Lonza (Basel, Switzerland), and Jurkat was obtained from the ATCC cell bank (Manassas, VA, USA). Cell culture media were obtained from Thermo Fisher Scientific (Waltham, MA, USA).

2.2 Preparation of the thermoresponsive cationic block copolymer brush

A thermoresponsive cationic block copolymer brush with various DMAPAAm compositions was prepared using two steps of ATRP (Fig. 1A). Silica beads (64–210 µm) were sieved to the fractions of 75–106 µm, 106–150 µm, and 150–210 µm using sieves with 106-µm and 150-µm meshes. Then, 50 g of the sieved beads of each fraction were washed with hydrochloride at 90°C for 3 h. Then, the beads were filtrated, rinsed with pure water, and then with acetone, respectively. Afterward, they were dried at 150°C for 7 h using a drying vacuum oven (DP200, Yamato, Tokyo).

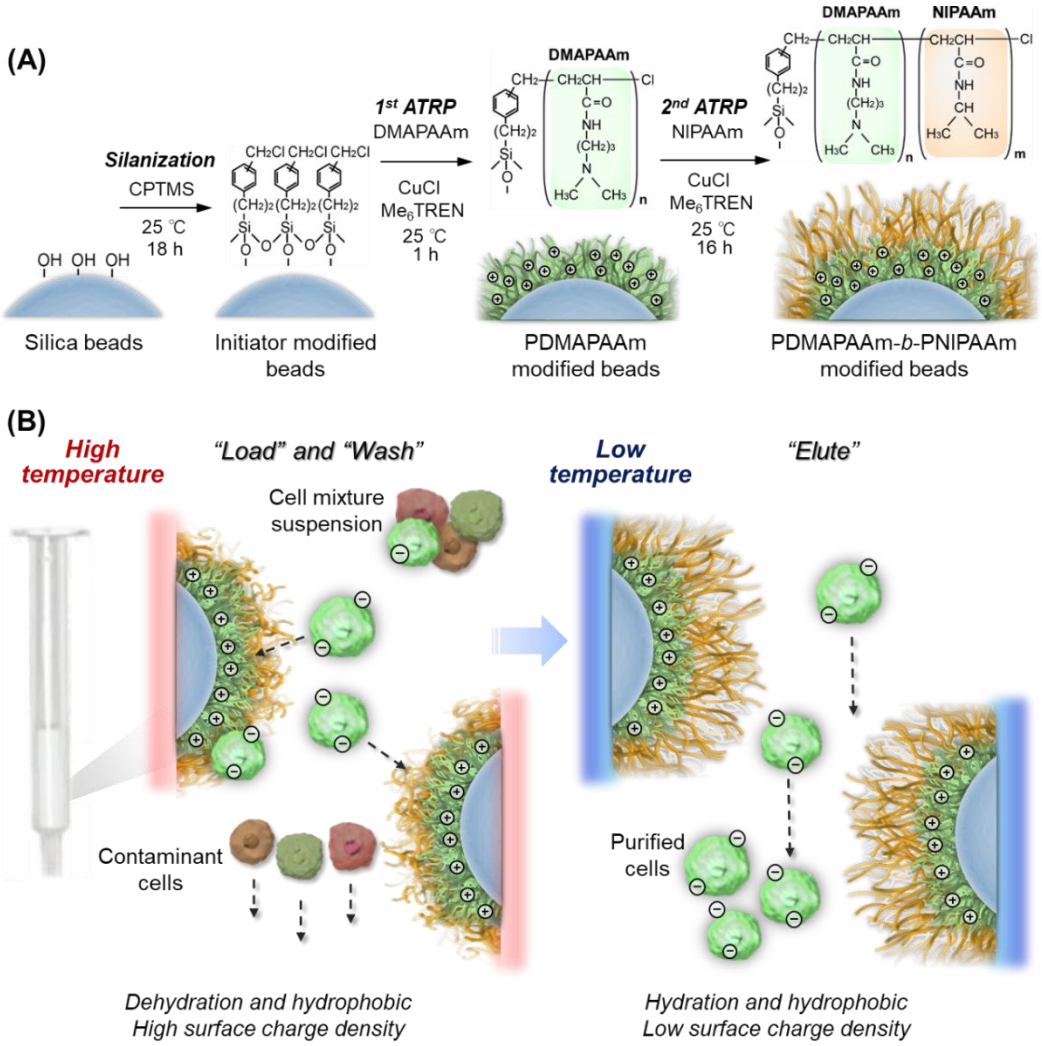

Fig. 1. Schematic illustration of: (A) the preparation of the thermoresponsive cationic copolymer brush as a column packing material. (B) column separation of a mesenchymal stem cell using the beads packed column.

An ATRP initiator, CPTMS, was immobilized through a silane coupling reaction (Fig. 1A). The beads (10g) were put in a 500-mL flask and humidified at a relative humidity of 60% for 3 h by flowing humidified nitrogen gas in the flask. Then, CPTMS (12.4 mL, 0.05 mol) was dissolved into 300 mL of toluene, and the CPTMS solution was poured into the flask. The silane coupling reaction was subsequently started at 25°C for 16 h with continuous stirring. After the reaction, the silica beads were filtered and rinsed with acetone. Then, they were dried at 110°C for 3 h using the drying vacuum oven.

PDMAPAAm was modified on the silica beads through the first ATRP. The amount of PDMAPAAm on the silica beads was modulated by the amount of the DMAPAAm monomers in the ATRP reaction from 0.103 mmol to 4.10 mmol. In the case of the polymerization of 0.103 mmol of DMAPAAm, DMAPAAm (15.9 mg, 0.103 mmol) were dissolved in 40 mL of 2-propanol in a 100-mL flask. The solution was deoxygenated by argon gas bubbling for 20 min. CuCl (26.22 mg, 0.26 mmol) and Me_6TREN (68.00 mg, 0.30 mmol) were dissolved in the solution under an argon gas atmosphere. Then, the flask was sealed and placed in a glove bag. CPTMS immobilized silica beads (3.0 g) were put into a 50-mL glass vessel, which was then placed in the same glove bag. The oxygen in the glove bag was removed by repeated vacuuming and argon gas flowing three times. Then, the ATRP reaction solution was poured into the silica beads in the glass vessel, and α-chloro-*p*-xylene (1.75 μL, 1.32×10^{-5} mol) was added to the reaction solution. The glass vessel was sealed in the glove bag, and the reaction proceeded at 25°C for 1 h with continuous shaking. After the reaction, the silica beads were filtered and rinsed with acetone, and the beads were dried at 50°C for 3 h using the drying vacuum oven.

PDMAPAAm-*b*-PNIPAAm-grafted silica beads were prepared through the second ATRP reaction for the block copolymerization of NIPAAm from the PDMAPAAm-grafted silica beads. NIPAAm (4.60 g, 40.7 mmol) were dissolved in 40 mL of 2-propanol in a 100-mL flask, and the solution was deoxygenated by argon gas bubbling for 20 min. CuCl (26.22 mg, 0.26 mmol) and Me_6TREN (68.00 mg,

0.30 mmol) were dissolved in the solution under an argon gas atmosphere. Then, the flask was sealed and placed in a glove bag. PDMAPAAm-grafted silica beads (2.8 g) were put in a 50-mL glass vessel, which was then placed in the same glove bag. The oxygen in the glove bag was removed by repeated vacuuming and argon gas flowing three times. Then, the ATRP reaction solution was poured into the silica beads in the glass vessel, and α-chloro-*p*-xylene (1.75 μL, 1.32×10^{-5} mol) was added to the reaction solution. The glass vessel was sealed in the glove bag, and the reaction proceeded at 25°C for 16 h with continuous shaking. After the reaction, the silica beads were filtered and rinsed with acetone, and the beads were washed with a mixture solution of 50 mM EDTA and methanol (1:1) with sonification. Then, the beads were filtered, rinsed with pure water, and dried at 50°C for 3 h using the drying vacuum oven.

For comparison, PNIPAAm homopolymer modified silica beads were prepared through the same ATRP procedure as the second ATRP, except that the CPTMS-modified beads were used in place of the PDMAPAAm-modified beads.

The prepared beads were named as PD X -***b***-PN, where X is the molar percentage of DMAPAAm to NIPAAm in the ATRP reaction.

2.3 Characterization of the thermoresponsive cationic block copolymer brush

The prepared polymer-modified silica beads were characterized using a Carbon/Hydrogen/Nitrogen (CHN) elemental analysis, attenuated total reflection/Fourier-transform infrared spectroscopy (ATR/FTIR), and field emission scanning electron microscopy (FE-SEM).

The carbon composition of the prepared beads was measured using a CHN elemental analyzer (PE2400, PerkinElmer, Waltham, MA, USA). The amount of initiators and polymers on the silica beads

was estimated through the carbon composition of the beads, and the amount of the immobilized initiators on the silica beads was estimated as follows.

$$\frac{\%C_I}{\%C_I(calcd)\times(1-\%C_I/\%C_I(calcd))\times S}, \quad (1)$$

where $\%C_I$ is the increase in the carbon percentage of the initiator-modified beads through the silane coupling reaction, $\%C_I$ (*calcd*) is the calculated percentage of carbon in the CPTMS, and *S* is the surface area of the beads (475 m^2/g). The amount of PDMAPAAm was obtained using the following equation.

$$\frac{\%C_D}{\%C_D(calcd)\times(1-\%C_D/\%C_D(calcd)-\%C_I/\%C_I(calcd))\times S}, \quad (2)$$

where $\%C_D$ is the increase in the percentage of carbon in the PDMAPAAm-modified beads through the first ATRP, and $\%C_D$ (*calcd*) is the calculated percentage of carbon in DMAPAAm. The amount of the modified PNIPAAm segment through the second ATRP was estimated as follows.

$$\frac{\%C_N}{\%C_N(calcd)\times(1-\%C_N/\%C_N(calcd)-\%C_D/\%C_D(calcd)-\%C_I/\%C_I(calcd))\times S}, \quad (3)$$

where $\%C_N$ is the increase in the percentage of carbon in the PDMAPAAm-*b*-PNIPAAm-modified beads through the second ATRP, and $\%C_N$ (*calcd*) is the calculated percentage of carbon in NIPAAm. The amount of modified block copolymers was obtained by summing the amounts of PDMAPAAm (eq (2)) and PNIPAAm (eq (3)).

The polymer modification of the silica beads on each ATRP was confirmed by ATR/FTIR using a FTIR-4700 (JASCO, Tokyo, Japan).

The surface morphology of the beads was observed by FE-SEM using an S-4700 (Hitachi High Technologies, Tokyo, Japan).

2.4 Cell elution from the beads packed column

The column was prepared by packing the beads into an empty solid-phase extraction column (inner diameter: 0.9 mm, length: 65 mm, total volume: 1.5 mL). A filter with 50 μm mesh was placed in the column, and the prepared beads (300 mg) were added afterward. A small amount of a mixture solvent of water: methanol = 1:1 was added to damp the packed beads. Then, the filter was placed on the packed beads in the column. The packed column was rinsed with a mixture solvent of water: methanol = 1:1, ethanol, and pure water.

The cells were cultured using the cell culture medium in Table S1. Before loading the cell suspension to the column, 5 mL of the cell culture medium, which were warmed at 37°C, were flowed through the column. Then, 1 mL of cell suspension (5.0×10^5 cells/mL) was passed by a cell strainer, and the cell suspension was introduced to the column at a flow rate of 1 mL/min using a syringe pump (YSP-202, YMC, Kyoto, Japan) while maintaining the column temperature at 37°C using a column temperature controller (Senshu Scientific, Tokyo, Japan). The eluted fraction from the column was defined as "Load." Then, the cell culture medium (1 mL) was flowed to the column at 37°C at a flow rate of 1 mL/min so as to rinse the nonadsorbed cells from the column. The flowing process was performed two times. Each eluted fraction was defined as "Wash." Then, the column was cooled at 4°C, and 1 mL of the cell culture medium, which was cooled at 4°C, was flowed into the column using a syringe pump at a flow rate of 9 mL/min. The flowing process was performed three times. Each eluted fraction was defined as "Elute," and the amount of cells in each fraction was measured using a cell viability analyzer (Vi-CELL XR, Beckman Coulter, Pasadena, CA, USA). The cell recovery ratio was obtained through the ratio of eluted cells to loaded cells.

A cell separation experiment was performed using a similar procedure. A mixture of MSC and BM-$CD34^+$ was prepared by mixing each cell suspension with a cell density of 5.0×10^5 cells/mL. The cell suspension (1 mL) was flowed into the column at 37°C at a flow rate of 1 mL/min, and the eluted

fraction was defined as “Load” fraction. Then, the cell culture medium (1 mL) was flowed into the column at 37°C at a flow rate of 1 mL/min, and this process was repeated four times. Each eluted fraction was mixed, and the mixed fraction was defined as “Wash.” Then, 1 mL of the cooled cell culture medium was flowed into the column, and the adsorbed cells were eluted. Elution was then performed five times. The eluted fraction was mixed, and the mixed fraction was defined as “Elute.” The cell composition of each fraction was measured through flow cytometry with the modification of the MSCs with CD73-PE antibodies.

The cell viability of the eluted fraction was observed using a trypan blue exclusion test with a cell viability analyzer (Vi-CELL XR). The viability of cells before the column loading were also observed as control.

The cell proliferation ability of the recovered MSC from the column was investigated by culturing the cells in a 24-well cell culture plate with a predetermined culture period of four days. Then, the cells were recovered with trypsin and were counted using a cell viability analyzer (Vi-CELL XR). The cells before the column loading were cultured and used as control.

The differentiation ability of the recovered MSCs from the column was evaluated using osteogenic and adipogenic differentiations. The osteogenic differentiation of the MSCs was performed by culturing with an osteogenic differentiation medium for 9 days, where the medium was replaced every four days. The osteogenic differentiation was confirmed through alizarin red staining. The adipogenic differentiation of the MSCs was performed by culturing with an adipogenic differentiation medium for 12 days, where the medium was replaced every four days. The adipogenic differentiation was confirmed by oil red O staining.

3. Results and discussion

3.1 Characterization of the thermoresponsive cationic block copolymer brush on the silica beads

PDMAPAAm-*b*-PNIPAAm brush-modified beads were prepared through two steps of surface-initiated ATRP. The prepared beads were characterized using a CHN elemental analysis to estimate the amount of the immobilized initiators and polymers on the silica beads (Table 1). A higher carbon composition was observed on the initiator-immobilized silica beads than on the unmodified silica beads, as the CPTMS was immobilized on the silica beads through the silane coupling reaction. The amount of immobilized CPTMS was 2.99 μmol/m^2, which is almost the same as the silanol group density on the silica beads surface.[63] These results indicate that most of the silanol groups on the silica beads were used for the coupling reaction with CPTMS. The carbon and nitrogen compositions of the PDMAPAAm-modified silica beads (PD0.25, PD0.5, PD1, and PD10) exhibited a higher carbon composition compared with the initiator-immobilized silica beads, indicating that PDMAPAAm were modified in the first step of the ATRP reaction. The amount of the modified PDMAPAAm increased with the increase in the DMAPAAm monomers in the first ATRP reaction, as this increase enhanced the polymerization rate, leading to an increase in the amount of the modified PDMAPAAm on the silica beads. Higher carbon and nitrogen compositions were observed on the PDMAPAAm-*b*-PNIPAAm-modified silica beads compared with the PDMAPAAm-modified silica beads, indicating that the second ATRP reaction successfully grafted PNIPAAm segments on PDMAPAAm. The amount of modified block copolymers, PDMAPAAm-*b*-PNIPAAm, was relatively small compared with the previously reported polymer brush-modified silica beads due to the small pore diameter of the beads (6 nm).[64, 65] In the previous study, silica beads with a pore diameter of 30 nm were used. Thus, the polymers were grafted inside the pores of the beads through surface-initiated polymerization.[66, 67] However, the pore diameter of the silica beads in this study is small. Thus, effective copolymer grafting inside the pores was not performed, whereas a copolymer modification on the outer

surfaces of the beads was performed, leading to a relatively smaller grafted amount of copolymers on the silica beads. However, in this study, the copolymer-grafted silica beads were used as packing materials of the cell separation column. Thus, copolymer modification inside the pores was not required as the cells cannot enter inside them.

Table 1. Characterization of the prepared thermoresponsive cationic block copolymer-modified beads.

Code[a)]	Elemental composition (%) [b)]			Immobilized initiator ($\mu mol/m^2$) [c)]	Grafted polymer (mg/m^2) [c)]
	C	H	N		
Unmodified silica beads	0.21 ± 0.03	0.64 ± 0.31	0.04 ± 0.03		
Initiator-immobilized silica beads	12.19 ± 0.16	0.67 ± 0.04	0.02 ± 0.01	2.99	
PN	16.75 ± 0.82	1.47 ± 0.17	1.40 ± 0.08		0.208
PD0.25	12.51 ± 0.07	0.92 ± 0.06	0.42 ± 0.00		0.014
PDN0.25-*b*-PN	17.68 ± 0.33	1.69 ± 0.06	1.60 ± 0.02		0.257
PD0.5	12.89 ± 0.16	0.94 ± 0.11	0.39 ± 0.02		0.030
PD0.5-*b*-PN	17.05 ± 0.34	1.46 ± 0.05	1.43 ± 0.04		0.225
PD1	13.00 ± 0.09	0.93 ± 0.09	0.44 ± 0.02		0.035
PD1-*b*-PN	17.46 ± 0.07	1.45 ± 0.05	1.39 ± 0.03		0.247
PD10	14.33 ± 0.15	1.05 ± 0.03	1.02 ± 0.01		0.096
PD10-*b*-PN	18.39 ± 0.77	1.68 ± 0.13	1.89 ± 0.07		0.299

a) The code of the prepared thermoresponsive copolymer brush-modified beads was determined as "PDX-*b*-PN", where X is the molar percentage of DMAPAAm to that of NIPAAm in ATRP. b) Determined by the CHN elemental analysis. c) Estimated using the carbon composition.

Polymer modification through ATRP was also confirmed by observing the FTIR spectrum (Fig. 2). Two additional peaks were observed at approximately 1550 and 1645 cm^{-1} on the PNIPAAm-modified, PDMAPAAm-modified, and PDMAPAAm-*b*-PNIPAAm-modified beads. These peaks were attributed to the C=O stretching and N-H bending vibrations of the amide group of DMAPAAm and NIPAAm. Thus, these results indicate that polymer modification was successfully performed through ATRP.

SEM observations of the prepared silica beads were performed after each reaction step to confirm the morphology of the silica beads (Fig. 3). The silica beads maintained their spherical morphology after the silane coupling reaction and the first and second ATRP reactions. These results indicate that the reaction steps did not deform the silica beads.

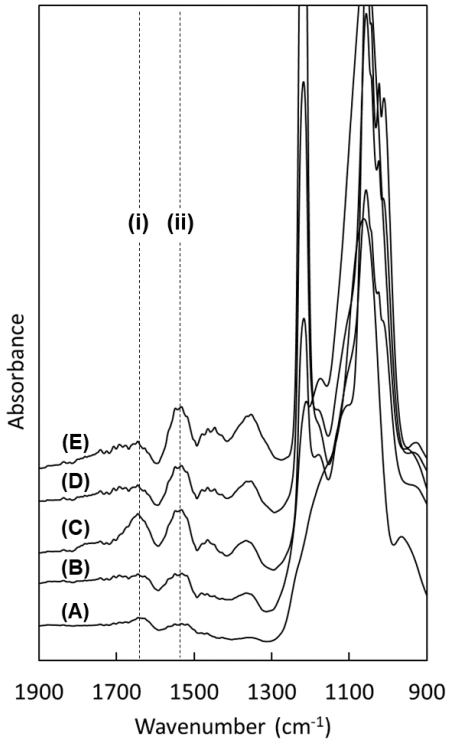

Fig. 2. Fourier-transform infrared spectroscopy (FTIR) spectra of the prepared beads. (A) Unmodified silica beads (5 mm), (B) initiator-modified silica beads, (C) PNIPAAm-modified beads (PN), (D) PDMAPAAm-modified silica beads (PD0.5), and (E) PDMAPAAm-*b*-PNIPAAm-modified beads (PD0.5-*b*-PN). The lines (i) and (ii) represent the peaks attributed to the C=O stretching and N-H bending vibrations, respectively.

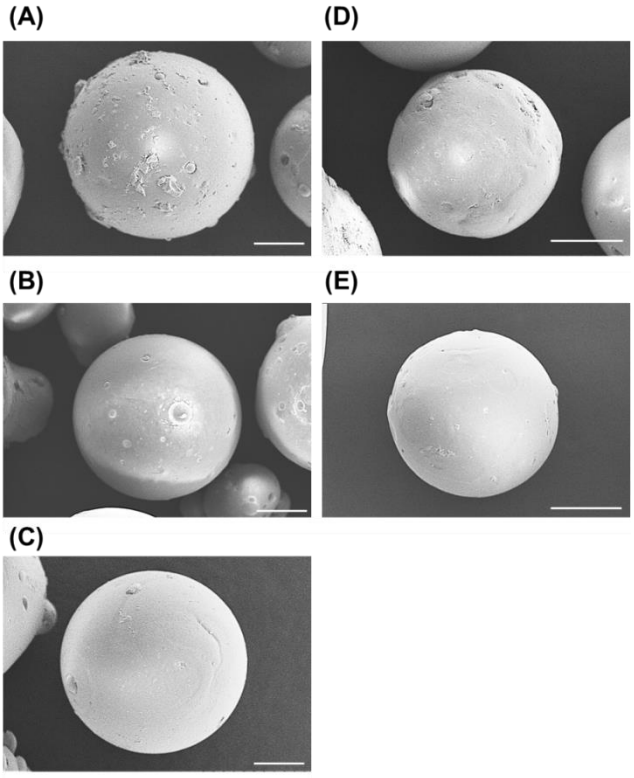

Fig. 3. Field emission scanning electron microscopy (FE-SEM) images of the prepared beads. (A) Unmodified beads, (B) initiator-modified beads, (C) PNIPAAm-modified beads (PN), (D) PDMAPAAm-modified silica beads (PD0.5), and (E) PDMAPAAm-*b*-PNIPAAm-modified beads (PD0.5-*b*-PN). Scale bars: 50 μm.

3.2 Cell elution behavior using the beads packed column

The prepared beads were packed into a syringe-type column. The cell elution behavior was observed using MSCs. At first, the proper bead size was investigated using two types of bead fractions as packing materials of the column. Two types of PNIPAAm-modified silica beads with diameters of 106–150 and 150–210 μm were used as packing materials, and the elution behavior of the MSCs was observed (Fig. 4). Both columns exhibited temperature-dependent cell elution. A larger cell elution was observed in the elute fraction at 4°C compared with the load and wash fractions at 37°C because of the temperature-modulated cell adsorption and desorption, which are attributed to the hydrophobicity change of PNIPAAm. On the wash and elute fractions at 37°C, the bead surface became hydrophobic

due to the dehydration of the modified PNIPAAm, leading to cell adsorption on the beads. On the contrary, at 4°C, the PNIPAAm on the beads became hydrophilic, and the adsorbed cells were detached from the bead surface, leading to the elution of the cells from the column. A larger elution was observed on the 150–210-μm beads packed column compared with the 106–150-μm beads packed column, which is due to the gaps between the cells among the packed beads in the column. The cells were flowed through the gaps of the packed beads in the column. In the case of the 106–150-μm beads packed column, the gaps were not adequate for flowing cells. Thus, a quite low cell elution ratio was observed on the 106–150-μm beads packed column. These results indicate that 150–210-μm beads are more suitable for packing column materials than 106–150-μm beads.

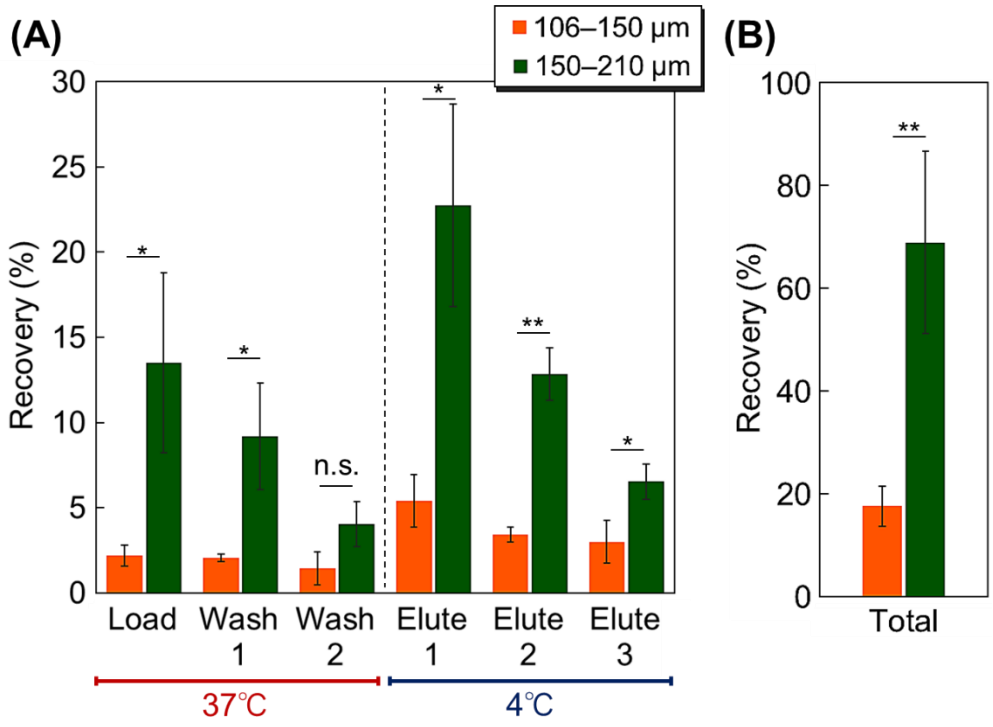

Fig. 4. Elution behavior of the mesenchymal stem cells from the columns using two types of beads grafted with PNIPAAm (n = 3). (A) Elution behavior of each fraction. (B) Total recovery ratio of the MSCs from the column. (*: $P < 0.05$; **: $P < 0.01$; and n.s.: not significant).

To investigate the proper cationic composition of the modified copolymers, the MSC elution behavior was observed on the columns with various PDMAPAAm compositions (Fig. 5). On all the columns, MSCs were adsorbed at 37°C and eluted at 4°C because the temperature-responsive property of the PDMAPAm-*b*-PNIPAAm brush on the silica beads changes. At 37°C, the upper PNIPAAm segment in the block copolymer became hydrophobic due to dehydration, leading to the adsorption of MSCs on the copolymer. Also, the upper PNIPAAm segment was shrunk, and the cationic bottom PDMAPAAm layer was exposed, leading to enhanced cell adsorption through the electrostatic interaction attributed to the negatively charged property of MSCs, whose zeta potential was -24.5 mV (Table S2). These factors enhanced the cell adsorption on the copolymer brush at 37°C. On the contrary, at 4°C, the PNIPAAm segment in the block copolymer became hydrophilic due to hydration. Also, the PNIPAAm segment was extended, leading to the prevention of electrostatic interactions between the bottom PDMAPAAm segment of the block copolymer and the cells. These factors led to the detachment of the MSCs from the copolymer brush.

The previous report indicated that PDMAPAm-*b*-PNIPAAm brush-modified glass substrate can perform temperature-modulated selective adhesion and detachment of umbilical cord derived MSCs (UC-MSCs).[57] UC-MSCs interact with PDMAPAAm-*b*-PNIPAAm brush grafted glass cover slips at 37°C because of the electrostatic interaction between MSCs and bottom PDMAPAAm segment. Additionally, PNIPAAm segment in block copolymer brush becomes hydrophobic, leading to enhance adhesion of MSCs on copolymer brush. By reducing temperature, the PNIPAAm segment in the block copolymer brush hydrate and extend, leading to the selective detachment of UC-MSCs.[57] In the present study, bone marrow derived MSCs also adsorb to PDMAPAAm-*b*-PNIPAAm brush on silica beads in the same manner, although there is a difference between bone marrow derived MSCs and UC-MSCs.

At 37°C, during the load and wash fractions, the MSC adsorption was enhanced with the increase in the PDMAPAAm composition on the beads. In addition, at 4°C, in the elute fractions, the recovery ratio decreased with the increase in the PDMAPAAm composition due to the enhanced electrostatic interaction between the MSCs and copolymer brush. Thus, the electrostatic interaction between the cationic PDMAPAAm segment and MSC increased with the increase in the PDMAPAAm amount in the copolymer segment. Among all the columns, PD0.5-*b*-PN exhibited effective MSC adsorption at 37°C and elution at 4°C.

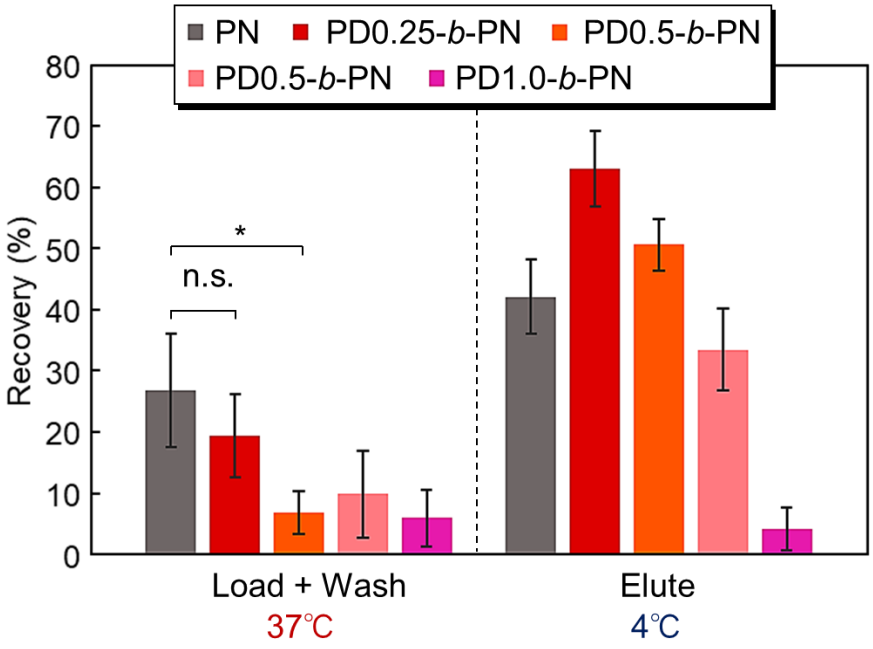

Fig. 5. Recovery ratio of the mesenchymal stem cells from the columns using various cationic copolymer composition-modified silica beads as packing materials (n=3). (*: $P < 0.05$ and n.s.: not significant).

The viability of the eluted MSCs from the various PDMAPAAm composition columns was observed using a trypan blue exclusion test (Fig. 6). The viability of the eluted MSC decreased with the increase in the PDMAPAAm composition. Especially, PD1.0-*b*-PN and PD10-*b*-PN exhibited low

viability. Cationic property of the copolymer-modified beads would lead to interaction with cell membrane proteins, and change three-dimensional structure of cell surface membrane proteins. Thus, the strong cationic property, such as PD1.0-*b*-PN and PD10-*b*-PN, disrupted the cell membrane, leading to eluted MSCs with low viability. On the contrary, PD0.25-*b*-PN and PD0.5-*b*-PN exhibited remaining cell viability, indicating that the relatively weak cationic property of the beads remained the structure of cell membrane. Thus, the PDMAPAAm composition was suitable below PD1.0-*b*-PN. The cell adhesion behaviors of the eluted MSCs from PN and PD0.5-*b*-PN on the tissue culture polystyrene dish were observed (Fig. S1). The MSCs from the eluted column exhibited a similar cell adhesion behavior to that before column loading. These results show that PN and PD0.5-*b*-PN maintained cell activity when passing through the column.

Considering the elution behavior of MSCs from the column and cell viability, the suitable column for the temperature-modulated MSC adsorption and detachment is PD0.5-*b*-PN.

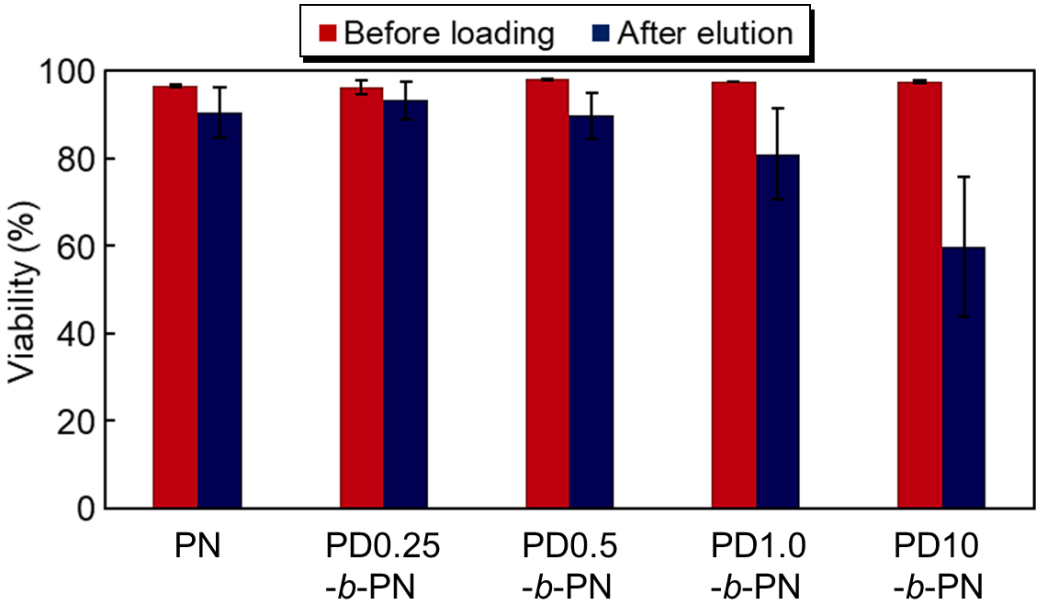

Fig. 6. Cell viability of the mesenchymal stem cells before loading and after elution from the columns with various cationic compositions of the copolymer.

Using the PD0.5-*b*-PN column, the elution behaviors of BM-CD34$^+$, NHDF, and Jurkat were observed and then compared with those of the MSCs (Fig. 7). BM-CD34$^+$ was derived from the bone marrow and then used as a model of contaminant cells in the bone marrow with the MSCs. NHDF was used as a model of adhesive cells, and Jurkat was used as a model of floating cells. The zeta potential of these cells was measured (Table S2). BM-CD34$^+$ and Jurkat exhibited large cell elution at 37°C, indicating that cells were not adsorbed on the block copolymer brush at 37°C. On the contrary, MSCs were adsorbed on the copolymer brush at 37°C, leading to the small elution of the MSCs at 37°C. This is probably due to the difference in the negative charge among the cells. The zeta potentials of BM-CD34$^+$ and Jurkat were −6.70 and −2.5, respectively. On the contrary, the zeta potential of the MSCs was −24.5 mV. Thus, the MSCs were adsorbed on the copolymer brush through relatively strong electrostatic interaction compared with BM-CD34$^+$ and Jurkat. NHDF exhibited a low elution ratio at both 37°C and 4°C, which is probably because of the NHDF intrinsic adhesive property. NHDF exhibited strong adhesive properties on the PNIPAAm-modified interfaces compared with the other types of cells.[30, 32, 57] The properties would cause strong adsorption of NHDF on the column at both 37°C and 4°C.

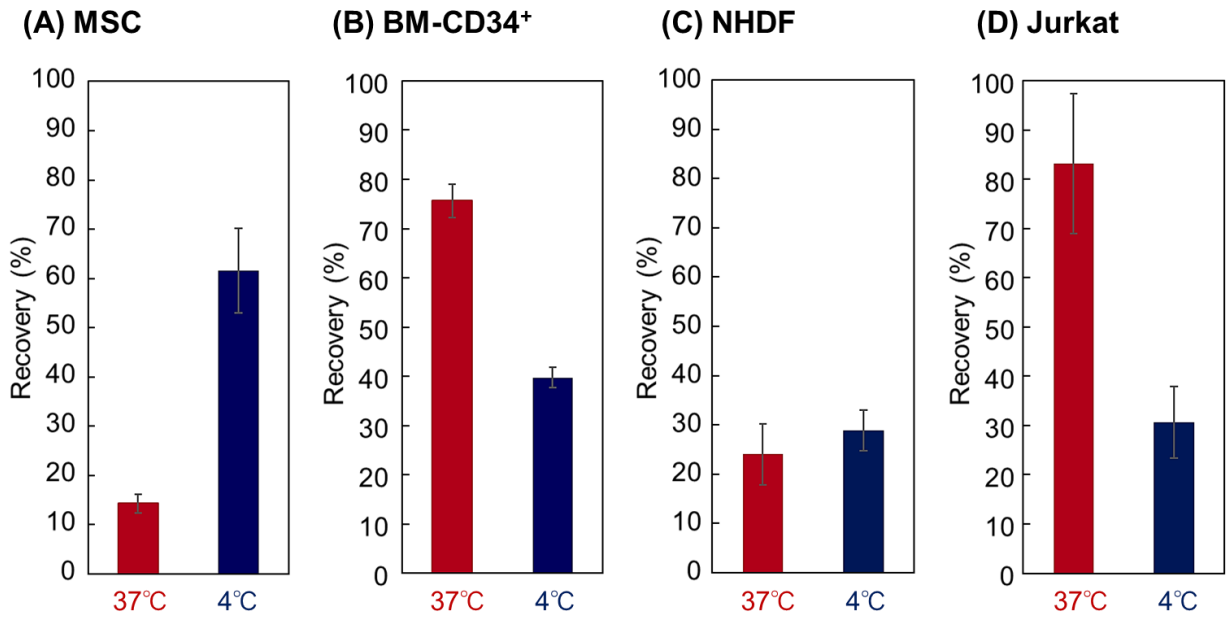

Fig. 7. Cell recovery ratio through the PD0.5-*b*-PN column using a (A) mesenchymal stem cell, (B) BM-CD34$^+$, (C) fibroblast, and (D) Jurkat.

To investigate the cell separation efficiency of the column, the elution behavior of the mixture of MSCs and BM-CD34$^+$ was observed using the PD0.5-*b*-PN column (Fig. 8). The same amounts of MSCs and BM-CD34$^+$ were mixed together, and a mixed cell suspension was introduced to the column. At 37°C, the load and wash fractions contained a large composition of BM-CD34$^+$ and barely contained MSCs, as the electrostatic interaction between the copolymer and BM-CD34$^+$ was relatively low compared with that of the MSCs. By reducing the temperature to 4°C, the elute fraction contained a large composition of MSCs, as the adsorbed MSCs on the copolymer brush were detached due to the hydration and extension of the PNIPAAm segment of the copolymer after lowering the temperature, leading to the elution of the MSCs from the column. This result indicates that the developed PD0.5-*b*-PN column separated the MSCs and other contaminant cells in the bone marrow by simply changing the column temperature. The purity of the MSCs is approximately 80%, which is not relatively

high compared to that of the purification of MSCs through fluorescent activated cell sorting (FACS) and magnetic activated cell sorting (MACS). However, the developed temperature-responsive cell separation column can purify the MSCs without modifying cell surfaces, which is advantage for the utilization of purified MSCs for cell transplantation therapy. This is because the cell modification process such as FACS or MACS would rescue cell's intrinsic property leading to reduced cell therapeutic effect after transplantation.

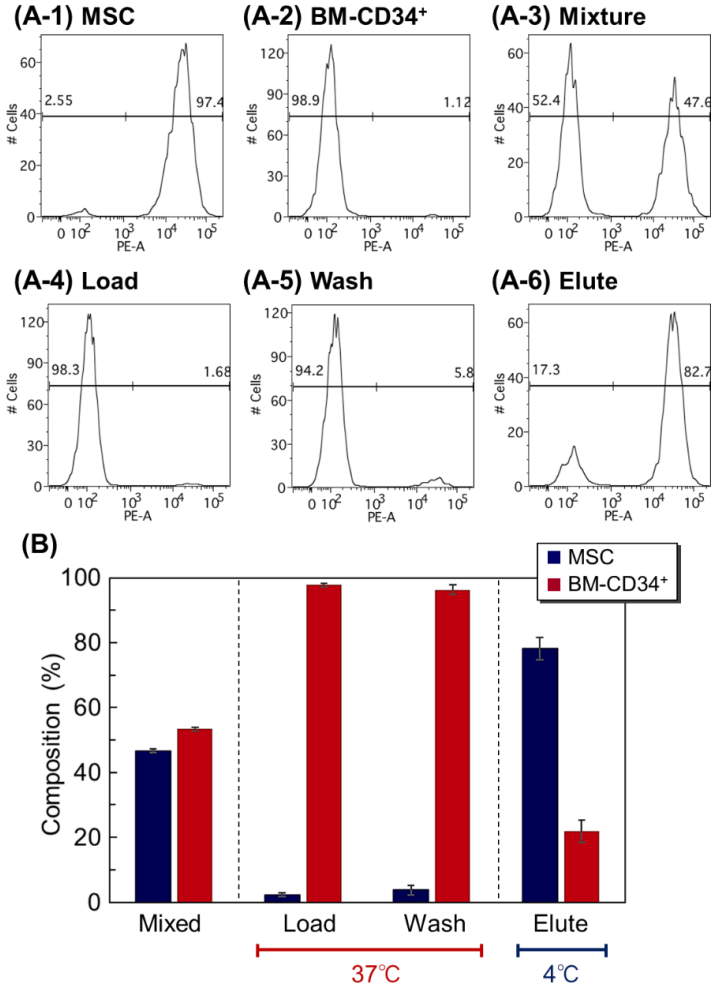

Fig. 8. Cell separation using the PD0.5-*b*-PN column by applying the mixture of MSC and CD-34$^+$. (A) Representative data of the flow cytometry analysis of each fraction. (A-1) MSC, (A-2) BM-CD34$^+$, (A-3) cell mixture of MSC and BM-CD34$^+$, (A-4) load fraction at 37°C, (A-5) wash fraction at 37°C, and (A-6) elute fraction at 4°C. (B) Cell composition of each fraction through the PD0.5-*b*-PN column.

The cell proliferation and differentiation of the recovered MSCs from the column were observed (Fig. S2 and Fig. 9) to investigate their cellular activities. The recovered MSCs from the PD0.5-*b*-PN column in the elute fraction were seeded and cultured on the cell culture dish, and the cell number at the predetermined culture period was observed. The recovered MSCs from the column exhibited a similar proliferation ability to that without column loading (Fig. S2). Also, the differentiation ability of the recovered MSCs from the column was investigated through osteogenic and adipogenic differentiations of the MSCs (Fig. 9). The recovered MSCs from the PD0.5-*b*-PN column in the elute fraction were differentiated by culturing with the osteogenic and adipogenic differentiation mediums. The alizarin red S staining in the osteogenic-differentiated MSCs indicated that the recovered MSCs were differentiated to osteoblast as similar as control MSCs, which were not passed through the column (Fig. 9). In addition, osteocalcin was observed in MSCs after osteogenic differentiation (Fig. S3). Additionally, the oil red O staining in the adipogenic-differentiated MSCs exhibited similar adipogenic differentiation to the control MSCs, which were not passed through the column. These results indicate that the recovered MSCs from the column maintained proliferation and differentiation abilities.

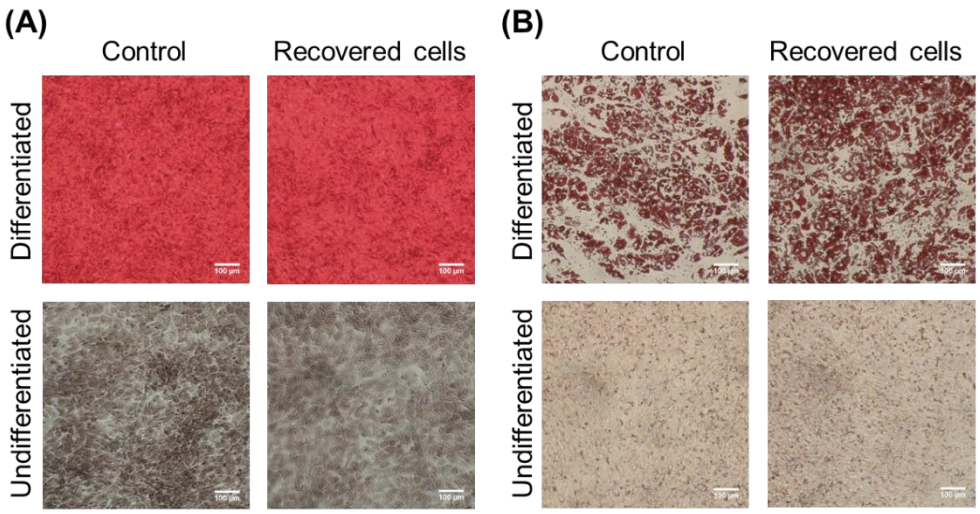

Fig. 9. Evaluation of the differentiation potency of the recovered cells by (A) the osteogenic differentiation of the mesenchymal stem cells with the staining alizarin red S and (B) the adipogenic differentiation of the MSCs with oil red O staining. Scale bar: 100 μm

Overall, the developed thermoresponsive cationic block copolymer brush-modified beads packed column in this study could modulate MSC adsorption and elution by changing the surface hydrophobicity of beads and the electrostatic interactions between copolymers and cells. Using these properties, MSCs can be simply separated by changing the temperature while maintaining cellular activities, such as viability, proliferation ability, etc. Thus, the developed columns in this study can be useful cell separation tools for MSCs.

4. Conclusions

In this study, we developed temperature-modulated MSC separation columns using thermoresponsive cationic block copolymer brush-modified beads as packing materials. A thermoresponsive cationic block copolymer, PDMAPAAm-*b*-PNIPAAm brush, was prepared on silica beads through a two-step ATRP reaction. At 37°C, the copolymer brush-modified beads packed column exhibited MSC adsorption through a hydrophobic interaction between the upper PNIPAAm segment in

the copolymer brush and the cells. In addition, the exposed bottom cationic DMAPAAm segment with the shrinking of the PNIPAAm segment enhanced the MSC adsorption, as the MSCs were negatively charged. The proper amount of PDMAPAAm in the copolymer was determined by changing the composition of the PDMAPAAm segment in the copolymer brush. The PD0.5-*b*-PN brush exhibited effective temperature-modulated MSC adsorption and desorption while maintaining cell viability. Using the PD0.5-*b*-PN column, the separation of MSCs and the BM-$CD34^+$ cells was performed. At 37°C, most of the BM-$CD34^+$ cells were eluted from the column, whereas the MSCs were adsorbed on the column.

By reducing the temperature to 4°C, the adsorbed MSCs were eluted from the column. The differences in the cell adsorption properties on the column at each temperature led to the temperature-modulated separation of the MSCs. In addition, the recovered MSCs from the column maintained proliferation and differentiation abilities. Thus, the developed column in this study can be a useful MSC separation tool, as the MSCs could be simply separated by changing the temperature while maintaining the cellular activity without modifying the cell surfaces.

Acknowledgments

This research was partially supported by a Grant-in-Aid for Scientific Research (grant no. 19H02447 and 20H05233) from the Japan Society for the Promotion of Science and SENTAN (grant no. JPMJSN16B3) from the Japan Science and Technology Agency.

Conflict of interests

There are no conflicts of declare.

Electronic supplementary information

Supplementary data can be found in the online version.

REFERENCES

1. R. Langer and J. Vacanti, *Science*, 1993, **260**, 920-926.
2. P. Menasché, A. A. Hagège, M. Scorsin, B. Pouzet, M. Desnos, D. Duboc, K. Schwartz, J.-T. Vilquin and J.-P. Marolleau, *The Lancet*, 2001, **357**, 279-280.
3. T. Shin'oka, Y. Imai and Y. Ikada, *New England Journal of Medicine*, 2001, **344**, 532-533.
4. K. Nishida, M. Yamato, Y. Hayashida, K. Watanabe, N. Maeda, H. Watanabe, K. Yamamoto, S. Nagai, A. Kikuchi, Y. Tano and T. Okano, *Transplantation*, 2004, **77**, 379-385.
5. T. Iwata, M. Yamato, K. Washio, T. Yoshida, Y. Tsumanuma, A. Yamada, S. Onizuka, Y. Izumi, T. Ando, T. Okano and I. Ishikawa, *Regenerative Therapy*, 2018, **9**, 38-44.
6. M. Sato, M. Yamato, G. Mitani, T. Takagaki, K. Hamahashi, Y. Nakamura, M. Ishihara, R. Matoba, H. Kobayashi, T. Okano, J. Mochida and M. Watanabe, *npj Regenerative Medicine*, 2019, **4**, 4.
7. H. K. Salem and C. Thiemermann, *Stem Cells*, 2010, **28**, 585-596.
8. X. Wei, X. Yang, Z.-p. Han, F.-f. Qu, L. Shao and Y.-f. Shi, *Acta Pharmacol Sin*, 2013, **34**, 747-754.
9. K. Kim, S. Bou-Ghannam, S. Kameishi, M. Oka, D. W. Grainger and T. Okano, *J. Control. Release*, 2021, **330**, 696-704.
10. M. Madrigal, K. S. Rao and N. H. Riordan, *Journal of Translational Medicine*, 2014, **12**, 260.
11. M. Nakao, D. Inanaga, K. Nagase and H. Kanazawa, *Regenerative Therapy*, 2019, **11**, 34-40.
12. M. Nakao, K. Kim, K. Nagase, D. W. Grainger, H. Kanazawa and T. Okano, *Stem Cell Research & Therapy*, 2019, **10**, 353.
13. N. Kaibuchi, T. Iwata, M. Yamato, T. Okano and T. Ando, *Acta Biomater.*, 2016, **42**, 400-410.
14. Y. Kato, T. Iwata, S. Morikawa, M. Yamato, T. Okano and Y. Uchigata, *Diabetes*, 2015, **64**, 2723-2734.
15. A. Imafuku, M. Oka, Y. Miyabe, S. Sekiya, K. Nitta and T. Shimizu, *STEM CELLS Translational Medicine*, 2019, **8**, 1330-1341.
16. N. Gandra, D.-D. Wang, Y. Zhu and C. Mao, *Angew. Chem. Int. Ed.*, 2013, **52**, 11278-11281.
17. N. Shomali, T. Gharibi, G. Vahedi, R. N. Mohammed, H. Mohammadi, S. Salimifard and F. Marofi, *Journal of Cellular Physiology*, 2020, **235**, 4120-4134.
18. A. Moldavan, *Science*, 1934, **80**, 188-189.
19. L. A. Herzenberg and L. A. Herzenberg, in *Handbook of Experimental Immunology*, ed. D. M. Weir, Blackwell Scientific Publication, Oxford, 1978, ch. 22, pp. 22.21-22.21.
20. S. Miltenyi, W. Müller, W. Weichel and A. Radbruch, *Cytometry*, 1990, **11**, 231-238.
21. J. C. Giddings, N. Barman Bhajendra and M.-K. Liu, in *Cell Separation Science and Technology*, American Chemical Society, 1991, vol. 464, ch. 9, pp. 128-144.
22. K. Kataoka, Y. Sakurai, T. Hanai, A. Maruyama and T. Tsuruta, *Biomaterials*, 1988, **9**, 218-224.
23. M. Kamihira and A. Kumar, in *Adv Biochem Engin/Biotechnol*, eds. A. Kumar, I. Galaev and B. Mattiasson, Springer Berlin / Heidelberg, 2007, vol. 106, pp. 173-193.
24. A. Mahara and T. Yamaoka, *Biomaterials*, 2010, **31**, 4231-4237.

25. M. Yamada, W. Seko, T. Yanai, K. Ninomiya and M. Seki, *Lab on a Chip*, 2017, **17**, 304-314.
26. A. Otaka, K. Kitagawa, T. Nakaoki, M. Hirata, K. Fukazawa, K. Ishihara, A. Mahara and T. Yamaoka, *Langmuir*, 2017, **33**, 1576-1582.
27. A. Otaka, A. Mahara, K. Ishihara and T. Yamaoka, *Journal of Micromechanics and Microengineering*, 2021, **31**, 045012.
28. K. Nagase, N. Mukae, A. Kikuchi and T. Okano, *Macromol. Biosci.*, 2012, **12**, 333-340.
29. K. Nagase, A. Kimura, T. Shimizu, K. Matsuura, M. Yamato, N. Takeda and T. Okano, *J. Mater. Chem.*, 2012, **22**, 19514-19522.
30. K. Nagase, Y. Hatakeyama, T. Shimizu, K. Matsuura, M. Yamato, N. Takeda and T. Okano, *Biomacromolecules*, 2013, **14**, 3423-3433.
31. K. Nagase, Y. Sakurada, S. Onizuka, T. Iwata, M. Yamato, N. Takeda and T. Okano, *Acta Biomater.*, 2017, **53**, 81-92.
32. K. Nagase, R. Shukuwa, T. Onuma, M. Yamato, N. Takeda and T. Okano, *J. Mater. Chem. B*, 2017, **5**, 5924-5930.
33. K. Nagase, R. Shukuwa, H. Takahashi, N. Takeda and T. Okano, *J. Mater. Chem. B*, 2020, **8**, 6017-6026.
34. K. Nagase, M. Shimura, R. Shimane, K. Hanaya, S. Yamada, A. M. Akimoto, T. Sugai and H. Kanazawa, *Biomaterials Science*, 2021, **9**, 663-674.
35. M. Nakayama, J. Akimoto and T. Okano, *Journal of Drug Targeting*, 2014, **22**, 584-599.
36. M. K. Jaiswal, M. Gogoi, H. Dev Sarma, R. Banerjee and D. Bahadur, *Biomaterials Science*, 2014, **2**, 370-380.
37. K. Nagase, M. Hasegawa, E. Ayano, Y. Maitani and H. Kanazawa, *Int J Mol Sci*, 2019, **20**, 430.
38. R. Nemoto, K. Fujieda, Y. Hiruta, M. Hishida, E. Ayano, Y. Maitani, K. Nagase and H. Kanazawa, *Colloids Surf. B*, 2019, **176**, 309-316.
39. A. Chilkoti, G. Chen, P. S. Stayton and A. S. Hoffman, *Bioconjugate Chemistry*, 1994, **5**, 504-507.
40. Y. G. Takei, T. Aoki, K. Sanui, N. Ogata, T. Okano and Y. Sakurai, *Bioconjugate Chemistry*, 1993, **4**, 42-46.
41. J. P. Chen, H. J. Yang and A. S. Hoffman, *Biomaterials*, 1990, **11**, 625-630.
42. T. Mori and M. Maeda, *Langmuir*, 2004, **20**, 313-319.
43. M. Ebara, J. M. Hoffman, A. S. Hoffman and P. S. Stayton, *Lab on a Chip*, 2006, **6**, 843-848.
44. J. M. Hoffman, P. S. Stayton, A. S. Hoffman and J. J. Lai, *Bioconjugate Chemistry*, 2015, **26**, 29-38.
45. Y.-J. Kim, S. H. Kim, T. Fujii and Y. T. Matsunaga, *Biomaterials Science*, 2016, **4**, 953-957.
46. M. Matsuura, M. Ohshima, Y. Hiruta, T. Nishimura, K. Nagase and H. Kanazawa, *Int J Mol Sci*, 2018, **19**, 1646.
47. H. Kanazawa, K. Yamamoto, Y. Matsushima, N. Takai, A. Kikuchi, Y. Sakurai and T. Okano, *Analytical Chemistry*, 1996, **68**, 100-105.
48. K. Nagase and T. Okano, *J. Mater. Chem. B*, 2016, **4**, 6381-6397.
49. K. Nagase, S. Kitazawa, S. Yamada, A. M. Akimoto and H. Kanazawa, *Analytica Chimica Acta*, 2020, **1095**, 1-13.
50. N. Yamada, T. Okano, H. Sakai, F. Karikusa, Y. Sawasaki and Y. Sakurai, *Makromol. Chem., Rapid Commun.*, 1990, **11**, 571-576.
51. Y. Akiyama, A. Kikuchi, M. Yamato and T. Okano, *Langmuir*, 2004, **20**, 5506-5511.
52. H. Takahashi, M. Nakayama, M. Yamato and T. Okano, *Biomacromolecules*, 2010, **11**, 1991-1999.

53. K. Nagase, M. Watanabe, A. Kikuchi, M. Yamato and T. Okano, *Macromol. Biosci.*, 2011, **11**, 400-409.
54. K. Komori, M. Udagawa, M. Shinohara, K. Montagne, T. Tsuru and Y. Sakai, *Biomaterials Science*, 2013, **1**, 510-518.
55. K. Nagase, N. Uchikawa, T. Hirotani, A. M. Akimoto and H. Kanazawa, *Colloids Surf. B*, 2020, **185**, 110565.
56. K. Nagase, Y. Hatakeyama, T. Shimizu, K. Matsuura, M. Yamato, N. Takeda and T. Okano, *Biomacromolecules*, 2015, **16**, 532-540.
57. K. Nagase, A. Ota, T. Hirotani, S. Yamada, A. M. Akimoto and H. Kanazawa, *Macromol. Rapid Commun.*, 2020, **41**, 2000308.
58. M. Ciampolini and N. Nardi, *Inorg. Chem.*, 1966, **5**, 41-44.
59. K. Okubo, K. Ikeda, A. Oaku, Y. Hiruta, K. Nagase and H. Kanazawa, *Journal of Chromatography A*, 2018, **1568**, 38-48.
60. K. Nagase, M. Watanabe, F. Zen and H. Kanazawa, *Analytica Chimica Acta*, 2019, **1079**, 220-229.
61. K. Nagase, S. Ishii, K. Ikeda, S. Yamada, D. Ichikawa, A. Akimoto, Y. Hattori and H. Kanazawa, *Scientific Reports*, 2020, **10**, 11896.
62. K. Nagase, Y. Umemoto and H. Kanazawa, *Scientific Reports*, 2021, **11**, 9976.
63. R. F. de Farias and C. Airoldi, *J. Therm. Anal. Calorim.*, 1998, **53**, 751-756.
64. K. Nagase, J. Kobayashi, A. Kikuchi, Y. Akiyama, H. Kanazawa and T. Okano, *Langmuir*, 2007, **23**, 9409-9415.
65. K. Nagase, J. Kobayashi, A. Kikuchi, Y. Akiyama, H. Kanazawa and T. Okano, *Langmuir*, 2008, **24**, 511-517.
66. K. Nagase, A. Mizutani Akimoto, J. Kobayashi, A. Kikuchi, Y. Akiyama, H. Kanazawa and T. Okano, *Journal of Chromatography A*, 2011, **1218**, 8617-8628.
67. K. Nagase, J. Kobayashi, A. Kikuchi, Y. Akiyama, H. Kanazawa and T. Okano, *ACS Appl. Mater. Interfaces*, 2012, **4**, 1998-2008.